Study of Remote Epitaxial Interaction Mechanism based on Magnetic Substrates

Mengxue Zhu

Shaoxing University, Shaoxing 312000, China

Abstract

In recent years, the remote epitaxy method has been widely used for the growth of high-quality two-dimensional thin film materials. The main idea is to realize the remote interaction between the polar substrate and the epitaxial layer by adding graphene as a buffer layer between the polar substrate and the epitaxial layer with the help of the translucency of graphene to the strongly polarized electric field. In this paper, by replacing the polar substrate with a nonpolar magnetic substrate in the remote epitaxy method, we propose a new idea of epitaxial growth: remote interaction based on the magnetization of the atoms of the epitaxial layer by the magnetic substrate through graphene. First principles calculations show that the remote magnetization of epitaxial bismuth metal by magnetic nickel (111) substrate through graphene significantly improves its adsorption on monolayer graphene, indicating the feasibility of this new remote epitaxial growth idea.

Keywords

Two-dimensional Material Growth; Remote Epitaxy; Magnetic Substrates; First-principles Calculations.

1. Introduction

Van der Waals (vdW) epitaxy is used for the preparation of flexible electronic devices as a method for growing metastable, high-quality two-dimensional layered materials [1,2]. The substrate surface used in vdW epitaxy is a two-dimensional layered material without hanging bonds, and the main interaction between the epitaxial layer and the substrate is a weak vdW interaction rather than a chemical bond interaction, thus significantly alleviating the problem of lattice mismatch between the epitaxial layer and the substrate layer in conventional heterogeneous epitaxy [2] and enabling the growth of single-crystal films with high quality.

Recently, a newer epitaxy method, i.e., remote epitaxy, has been used to efficiently grow a variety of thin films, such as GaAs [3], AlN [4], GaN [5-6], BaTiO3 [7] and SrTiO3 [8], ZnO [9], Cu [10], and Sn [11]. In remote epitaxy, a graphene layer is usually overlaid on a substrate material with electrode properties as a flat epitaxial substrate. The graphene layer is semitransparent to the electrostatic force of the substrate, and the polarization field of the polar substrate can cross the graphene layer to have remote polar interactions on the epitaxial layer.Kim et al. covered graphene layers on polar GaAs, GaN, and LiF substrates and grew high-quality GaAs, GaN, and LiF single-crystal films on graphene; while growing silicon or germanium on graphene-covered covalent silicon or germanium substrates would form low quality polycrystalline forms [3]. Therefore, polar substrate materials are usually used instead of covalently bonded substrate materials when using remote epitaxy for two-dimensional material growth.

Wu et al. successfully grew thin films of tin with a thickness of several atomic layers on a nonpolar copper (111) substrate covered by monolayer graphene (MLG) [11]. This new discovery not only

provides a new method for growing thin layers of metals, but also opens up a broad idea of remote epitaxy based on other remote interaction mechanisms than polar interactions.

In this paper, to explore the possibility of remote epitaxial growth on magnetic substrates, we calculated the adsorption of metallic bismuth on graphene-covered nickel(111) substrates using a first-principles calculation. The strong interaction and small lattice mismatch between metallic nickel and graphene, which can be easily removed to obtain independent graphene after growth, make metallic nickel one of the ideal substrates for epitaxial graphene. Our calculations show that the adsorption of graphene-covered magnetic nickel(111) substrate on epitaxial bismuth metal is significantly stronger than the adsorption of graphene monolayer on bismuth metal, confirming the remote interaction of magnetic substrate through graphene to magnetize epitaxial atoms.

2. Computational Models and Methods

In order to understand the remote epitaxial behavior of bismuth atoms on different substrates, we constructed two adsorption substrates, a monolayer graphene (MLG) and a monolayer graphene-covered nickel substrate (MLG/Ni(111)), with the specific adsorption configurations shown in Figure 1.
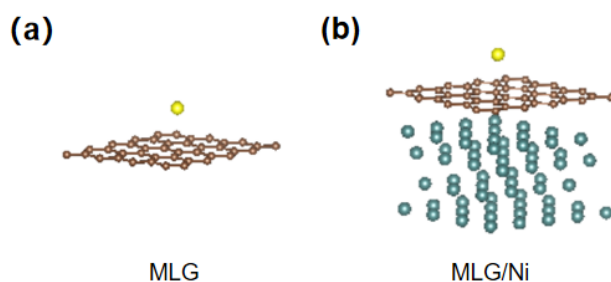

Figure 1. Side diagram of the adsorption model of bismuth atoms on (a) monolayer graphene substrate and (b) monolayer graphene-covered nickel substrate

According to the symmetry of the model, the bismuth atom has four possible adsorption sites on the MLG/Ni(111) substrate, which are denoted by top-A, top-B, bridge-G and hollow-H, respectively. As shown in Figure 2, the adsorption atom of the hollow-H site is located directly above the center of the ortho-hexagonal carbon ring of graphene, while the adsorption atom of the bridge-G site is located directly above the midpoint of the carbon-carbon bond of graphene, the top-A site and the top-B site are located directly above the carbon atoms of graphene, respectively, the carbon atom directly below the top-A site is located directly above the topmost nickel atom, and the top The carbon atom directly below the top-A site is located directly above the topmost nickel atom, and the carbon atom directly below the top-B site is located directly above the next top layer of nickel atoms. In Figure 2, the radii of the drawn nickel atoms decrease gradually from the top layer to the bottom layer in order to distinguish the nickel atoms in different layers.
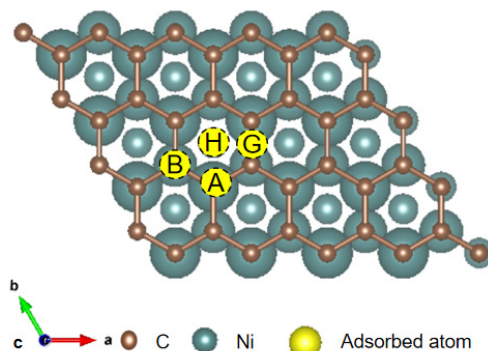

Figure 2. Four possible adsorption sites for bismuth atoms on MLG/Ni (111) substrates

We used the Vienna Ab initio Simulation Package (VASP) to obtain optimized adsorption structures and electronic properties using a first-principles calculation method based on density generalized function theory (DFT) [12]. We used the modified Perdew-Brucke-Ernerhof (RPBE) method [14-15] in the generalized gradient approximation (GGA) [13] to represent the electron exchange correlation function in our calculations. Given the importance of vdW interactions for adsorption, we used the DFT-D3 generalized function proposed by Grimme et al. in our calculations [16]. By convergence test calculations, we set the planar fluctuation energy cutoff energy to 520 eV and the k-point grid within the Brillouin zone to 6×6×1, obtaining a convergence accuracy of 0.01 eV/Å for the interatomic forces and 10^{-5} eV for the energy.

In modeling the supercell with nickel(111) as the substrate and graphene as the buffer layer for the adsorption structure, we used four layers of nickel atoms as the substrate, as shown in Fig. 1(b), and we set the lattice constant in the c-direction (perpendicular to the graphene plane direction) to 31 Å to ensure that the thickness of the vacuum layer inside the cell is greater than 15 Å. In the optimization calculation of this structure, we fixed the bottom two layers of nickel atoms and performed complete free relaxation for The rest of the nickel and carbon atoms were subjected to complete free relaxation. We performed DFT calculations for all adsorption structures and compared them, taking the lowest energy as the total energy of the adsorption structure. The adsorption energy of the adsorbed atoms is defined as Eads = Ead + Esub - Ead/sub, where Ead, Esub, and Ead/sub denote the isolated atom energy, isolated substrate energy, and atomic and substrate adsorption structure energies, respectively.

3. Effect of Magnetic Substrates on Adsorption

To investigate the remote interaction of magnetic substrates on epitaxial atoms, we calculated the adsorption of bismuth atoms on magnetic MLG/Ni(111) substrates and nonmagnetic MLG/Ni(111) substrates, respectively. We found that the adsorption energy increased by 0.16 eV when the bismuth atom was adsorbed on the non-magnetic MLG/Ni(111) substrate compared with that when it was adsorbed on the MLG substrate alone, while the adsorption energy increased by 0.33 eV when the bismuth atom was adsorbed on the magnetic MLG/Ni(111) substrate compared with that when it was adsorbed on the MLG substrate alone; that is, the bismuth atom on the magnetic substrate That is, the adsorption energy of the bismuth atom on the magnetic substrate increases by 0.17 eV compared to its adsorption energy on the non-magnetic substrate; therefore, the magnetic properties of the substrate play a pivotal role in its remote interaction with the epitaxial atoms.
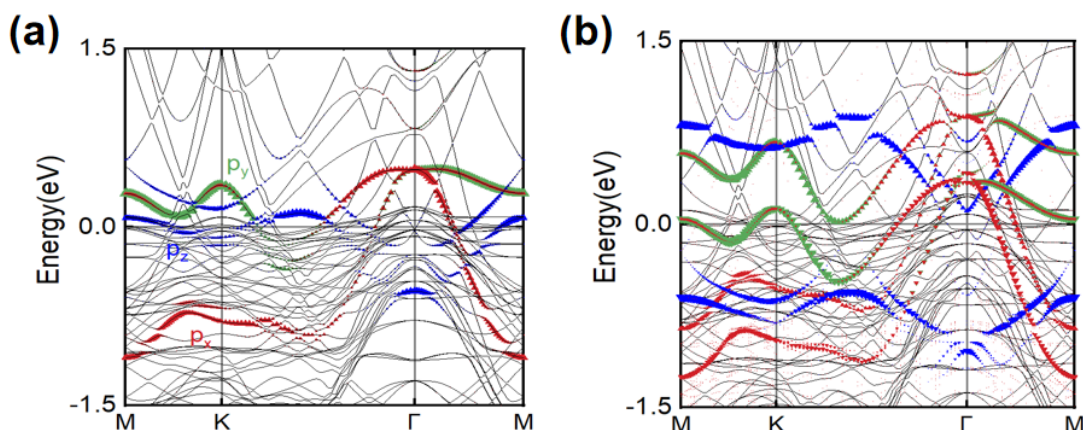

Figure 3. (a) Energy band diagram of non-magnetic Bi/MLG/Ni (111) adsorption structure; (b) Energy band diagram of magnetic Bi/MLG/Ni (111) adsorption structure

To reveal the mechanism of remote interaction of magnetic nickel substrates on bismuth atoms, we calculated the energy band structures of magnetic and non-magnetic adsorption structures separately, as shown in Figure 3. Figure 3(a) shows the energy band structure of the non-magnetic adsorption

structure, in which we have marked a half-occupied flat energy band consisting of pz orbitals of bismuth atoms near the Fermi energy (E=0) with blue lines. The half-occupied energy band is usually unstable, and magnetization will help to split this energy band into two spin-opposite energy bands and leave the Fermi energy, thus reducing the total energy of the structure. Figure 3(b) shows the energy band structure of the magnetically adsorbed structure, and we find that the flat energy band consisting of pz orbitals of the bismuth atom undergoes spin splitting (see the double blue line in the figure), in which the spin-up energy band moves to about 0.5 eV below the Fermi energy and reduces the total energy of the structure, thus revealing the remote mechanism of the magnetic substrate acting to reduce the energy of the structure by magnetizing the bismuth atom.

To further illustrate the magnetization of the epitaxial atoms by the magnetic substrate, in Fig. 4, we plot the fractional wave density of states (PDOS) of the isolated substrate, isolated graphene layer, isolated epitaxial atoms, and the p-orbitals of the substrate, graphene layer, and epitaxial atoms in the magnetically adsorbed structure, respectively, where the thin lines (light blue and light green) indicate the spin-up and spin-down PDOS, while the thick lines (dark blue and dark green) indicate the spin-up and spin-down PDOS of each part of the magnetically adsorbed structure. comparing the PDOS of the isolated structure, in the magnetically adsorbed structure, we find that although the PDOS of graphene has a less pronounced spin polarization (magnetization) effect, the PDOS of bismuth atoms has a very pronounced spin polarization, indicating that the magnetic substrate can penetrate through the graphene layer to the epitaxial atoms by magnetizing them. The remote interaction of the substrate on the epitaxial atoms is confirmed.
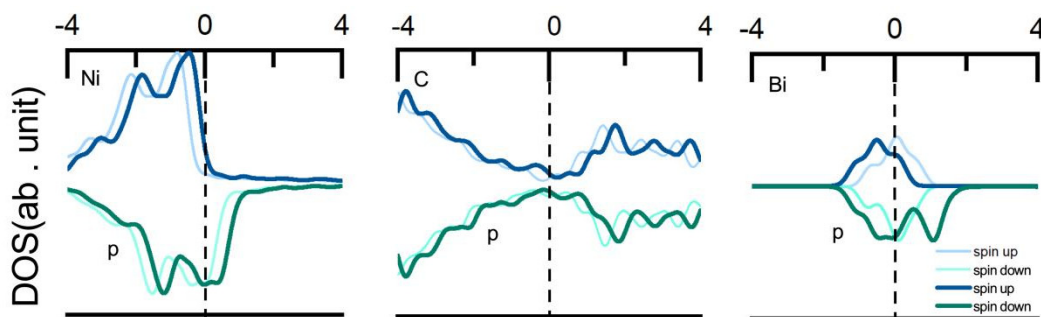

Figure 4. Isolated Ni (111) substrate, isolated graphene layer, isolated epitaxial atom, and fractional wave density of states in the p-orbitals of the substrate, graphene layer, and epitaxial atom in the Bi/MLG/Ni (111) magnetically adsorbed structure

4. Conclusion

We investigated the adsorption of metallic bismuth on graphene-covered nickel (111) substrates using a first-principles calculation method. The results show that the adsorption of graphene-covered magnetic nickel (111) substrate on epitaxial metallic bismuth is significantly stronger than that of graphene monolayer on metallic bismuth, and also stronger than that of nonmagnetic nickel (111) substrate on epitaxial metallic bismuth, confirming the remote interaction of magnetic substrate on epitaxial atoms through graphene. We reveal the remote interaction mechanism of the magnetic substrate by magnetizing the epitaxial atoms and thus reducing the total energy of the adsorbed structure by further investigating the energy band and the fractional wave state density of the adsorbed structure. Our study shows that magnetic substrates can be used for the remote epitaxial growth of thin films of metal atoms, foreshadowing the potential of remote epitaxial metal films on magnetic substrates for future applications in spintronics.

References

[1] Koma A, Yoshimura, K. Ultrasharp interfaces grown with Van der Waals epitaxy. Surface Science, (1986), 174(1-3), 556-560.

[2] Koma A. Papers presented at the International Workshop on Science and Technology of Thin Films for the 21st Century, Evanston, IL, USA, July 28–August 2, 1991 Van der Waals epitaxy—a new epitaxial growth method for a highly lattice-mismatched system[J]. Thin Solid Films, 1992, 216: 72-76.

[3] Kim H, Kim J C, Jeong Y, et al. Role of transferred graphene on atomic interaction of GaAs for remote epitaxy[J]. Journal of Applied Physics, 2021, 130(17): 174901.

[4] Qi Y, Wang Y, Pang Z, et al. Fast growth of strain-free AlN on graphene-buffered sapphire[J]. Journal of the American Chemical Society, 2018, 140(38): 11935-11941.

[5] Journot T, Okuno H, Mollard N, et al. Remote epitaxy using graphene enables growth of stress-free GaN[J]. Nanotechnology, 2019, 30(50): 505603.

[6] Qiao K, Liu Y, Kim C, et al. Graphene buffer layer on SiC as a release layer for high-quality freestanding semiconductor membranes[J]. Nano letters, 2021, 21(9): 4013-4020.

[7] Dai L, Zhao J, Li J, et al. Highly heterogeneous epitaxy of flexoelectric BaTiO3-δ membrane on Ge[J]. Nature Communications, 2022, 13(1): 2990.

[8] Yoon H, Truttmann T K, Liu F, et al. Freestanding epitaxial SrTiO3 nanomembranes via remote epitaxy using hybrid molecular beam epitaxy[J]. Science Advances, 2022, 8(51): eadd5328.

[9] Jeong J, Min K A, Kang B K, et al. Remote heteroepitaxy across graphene: Hydrothermal growth of vertical ZnO microrods on graphene-coated GaN substrate[J]. Applied Physics Letters, 2018, 113(23): 233103.

[10] Lu Z, Sun X, Xie W, et al. Remote epitaxy of copper on sapphire through monolayer graphene buffer[J]. Nanotechnology, 2018, 29(44): 445702.

[11] Wu H, Tang J, Liang Q, et al. A van der Waals epitaxial growth of ultrathin two-dimensional Sn film on graphene covered Cu (111) substrate[J]. Applied Physics Letters, 2019, 115(14): 141601.

[12] Kresse G, Furthmüller J. Efficient iterative schemes for ab initio total-energy calculations using a plane-wave basis set[J]. Physical review B, 1996, 54(16): 11169.

[13] Perdew J P, Burke K, Ernzerhof M. Generalized gradient approximation made simple[J]. Physical review letters, 1996, 77(18): 3865.

[14] Zhang Y, Yang W. Comment on "Generalized gradient approximation made simple" [J]. Physical Review Letters, 1998, 80(4): 890.

[15] Hammer B, Hansen L B, Nørskov J K. Improved adsorption energetics within density-functional theory using revised Perdew-Burke-Ernzerhof functionals[J]. Physical review B, 1999, 59(11): 7413.

[16] Grimme S, Antony J, Ehrlich S, et al. A consistent and accurate ab initio parametrization of density functional dispersion correction (DFT-D) for the 94 elements H-Pu[J]. The Journal of chemical physics, 2010, 132(15): 154104